Ratio spectra as a quality control tool for solar spectral UV measurements

G. Bernhard[1] and G. Seckmeyer

Fraunhofer Institute for Atmospheric Environmental Research, Garmisch-Partenkirchen, Germany

R. L. McKenzie and P. V. Johnston

National Institute of Water and Atmospheric Research, Lauder, New Zealand

Abstract. Spectra sampled by a UV spectroradiometer throughout the day are ratioed against a reference spectrum from the same instrument, typically the spectrum obtained at noon. The resultant ratios are a useful quality control tool that allows the detection of errors in the data acquisition of the instrument and shifts in its wavelength calibration. The method was applied to measurements of two high-quality spectroradiometers during the SUSPEN 1997 UV spectroradiometer intercomparison. Thus the wavelength calibration of both instruments was found to be stable to within ±0.01 nm. In both instruments, deficiencies were identified by this method, enabling remedial action to be taken.

1. Introduction

As a consequence of the observed decline in stratospheric ozone, increased levels of harmful solar UV radiation at the ground are expected [*McKenzie et al.*, 1994]. To quantify the current and future impacts of UV on the biosphere, accurate and spectrally resolved measurements of solar UV are required. Several international intercomparison campaigns of UV spectroradiometers held in recent years [e.g., *Gardiner et al.*, 1993; *Seckmeyer et al.*, 1994, 1995; *Webb*, 1997] have shown that UV data with the necessary accuracy can be obtained only if the instruments meet specific requirements and if rigorous quality control (QC) methods are applied. This includes a regular maintenance and calibration of the instruments as well as a careful inspection of the data. Here we present a QC tool that can be easily applied to detect variations in wavelength and short-term changes in radiometric stability. Examples of the use of the technique to determine wavelength errors, instrument stability, and useful dynamic range are given.

2. Method

A set of spectra measured by a UV spectroradiometer throughout the day are ratioed against a reference spectrum from the same instrument, typically the spectrum

[1]Now at Biospherical Instruments Inc., San Diego, California.

obtained at noon. Ideally, these ratios are smooth and free from the structure caused by the Sun's Fraunhofer lines, and thus instrumental features become clearly apparent. This characteristic makes ratio spectra useful as a QC tool. (The Fraunhofer lines in the solar spectrum are caused by absorptions by the various atoms in and above the Sun's photosphere.)

The method is suitable for detection of the following instrumental malfunctions: (1) shifts in the wavelength calibration over a day, (2) changes of an instrument's bandwidth, (3) spikes or distortions in an instrument's signal, and (4) nonlinearities of the detector or amplifier. Two examples of the latter are abrupt changes in the measured spectral irradiance that can occur if the high-voltage supply of a photomultiplier is altered during a scan or if an amplifier stage is changed. In addition, the method allows an estimation of the dynamic range and noise level.

Spectra from cloudless days are most amenable to this method. However, the technique can also be applied on cloudy days because apparent spectral features due to changing clouds are rather broad. This is because of the relatively slow rate of change of clouds during the scan period. For days with rapidly changing cloud conditions, it may be more appropriate to use the average of several spectra, or even the daily spectral dose as the reference. The wavelength stability over a longer time period can also be assessed if the same reference spectrum is used for several days.

3. Application of the Method

The method was applied to data sampled in July 1997 during an international intercomparison of UV spectroradiometers. The campaign was held in Nea Michan-

iona, Greece, within the framework of the European project "Standardisation of ultraviolet spectroradiometry in preparation of a European network" (SUSPEN). A total of 19 instruments took part, and measurements from two of these are used to demonstrate the method. One system is the "mobile UV spectroradiometer" of the Fraunhofer Institute for Atmospheric Environmental Research (IFU), Germany. The second instrument is from the National Institute of Water and Atmospheric Research (NIWA), New Zealand. Both instruments are based on Bentham double monochromators of type DTM300. Specifications of these systems are listed in Table 1. More details on the IFU radiometer and its normal mode of operation are given by *Bernhard et al.* [1997] and *Seckmeyer et al.* [1996].

The measurements of all 19 instruments were compared with average spectra that were calculated from the results of all instruments according to an algorithm described by *Webb* [1997]. (In brief, an average spectrum at a particular time is the median of the spectra measured at this time by a selection of several instruments.) The measurements of both the IFU and the NIWA spectroradiometers agreed with these average spectra to within ±2% for wavelengths above 300 nm and solar elevations above 15°, giving confidence in both systems. (Note that the average spectra were used only in the comparison of the measurements of the SUSPEN participants. The average spectra must not be confused with the reference spectra in the denominator of the ratio spectra proposed in this paper.)

Figure 1 shows the ratio spectra from both instruments, determined from measurements in the morning of July 5, 1997, to the noon spectra. With decreasing solar elevations, the light path through the atmosphere increases. As a consequence, the attenuation of solar radiation by Rayleigh and aerosol extinctions [*Iqbal*, 1983], and by absorption from atmospheric ozone, becomes more effective, leading to a gradual reduction of the ratios when the solar elevation decreases.

For wavelengths above 340 nm, the ratios show a moderate upward slope that is caused by the time of about 15 min to record a spectrum. (The scan rate during this campaign was chosen to allow time-synchronized measurements from all instruments participating in the campaign and was much slower than the normal scan rates of the IFU and NIWA instruments; see Table 1). Similarly, ratios with spectra taken during the afternoons decrease (not shown).

Because of ozone absorption, the ratio spectra at smaller solar elevations reduce rapidly at wavelengths below 340 nm. Structures in the ozone absorption cross section become clearly apparent in the ratio plots between 310 and 340 nm. Such features can be used to derive ozone column amounts using differential optical absorption spectroscopy (DOAS) and least squares minimization. The method has been applied for many years to the measurement of NO_2 and ozone in the violet region of twilight spectra [*McMahon and Simmons*, 1980; *McKenzie and Johnston*, 1983]. More recently, a wide range of trace gases has been measured by applying this technique in the UV-A region [*Kreher et al.*, 1997]. Since the absorption cross section of SO_2 shows prominent structures at wavelengths below 310 nm, a variation of the method could also be applied to measuring SO_2 in the UV-B region using daytime spectra (rather than twilight spectra). It should be emphasized that spectral features, which appear in ratio spectra because of absorption by atmospheric trace gases, do not restrict the applicability of ratio spectra as a quality control tool: In contrast to most instrumental features, absorption features are always apparent at the same wavelengths, and, in addition, they are dependent on air mass. Thus both kinds of structures can be distinguished.

Table 1. Specification of the NIWA and IFU UV Spectroradiometers

Specification	NIWA	IFU
Monochromator	Bentham DTM300, additive dispersion	Bentham DTM300, additive dispersion
Focal length, mm	300	300
Focal ratio	f/4.1	f/4.1
Gratings	Holographic, 2400 lines per millimeter	Holographic, 2400 lines per millimeter
Dispersion, nm/mm	0.675	0.675
Slit widths, mm	1.0, 1.5, 1.0[a]	0.74, 1.48, 0.74[a]
Bandwidth, nm	0.78	0.58 (nominal 0.5)
Entrance optics	PTFE diffuser, custom made, type Bo 5.8	PTFE diffuser, type P2[b]
Coupling	Quartz fiber bundle	Quartz fiber bundle
Detector	Photomultiplier EMI 9804 QA	Photomultiplier EMI 9205 QB
Amplification method	Analog	Lock-in
Normal sample step, nm	0.2	0.25
Normal wavelength range, nm	285 - 450	285 - 410
Normal scan period, s	200	450
Temperature stabilization	20.0° ± 0.5°C	20.0° ± 0.5°C

[a]Entrance-, intermediate- and exit-slit.
[b]See *Bernhard and Seckmeyer* [1997].

NIWA **IFU**
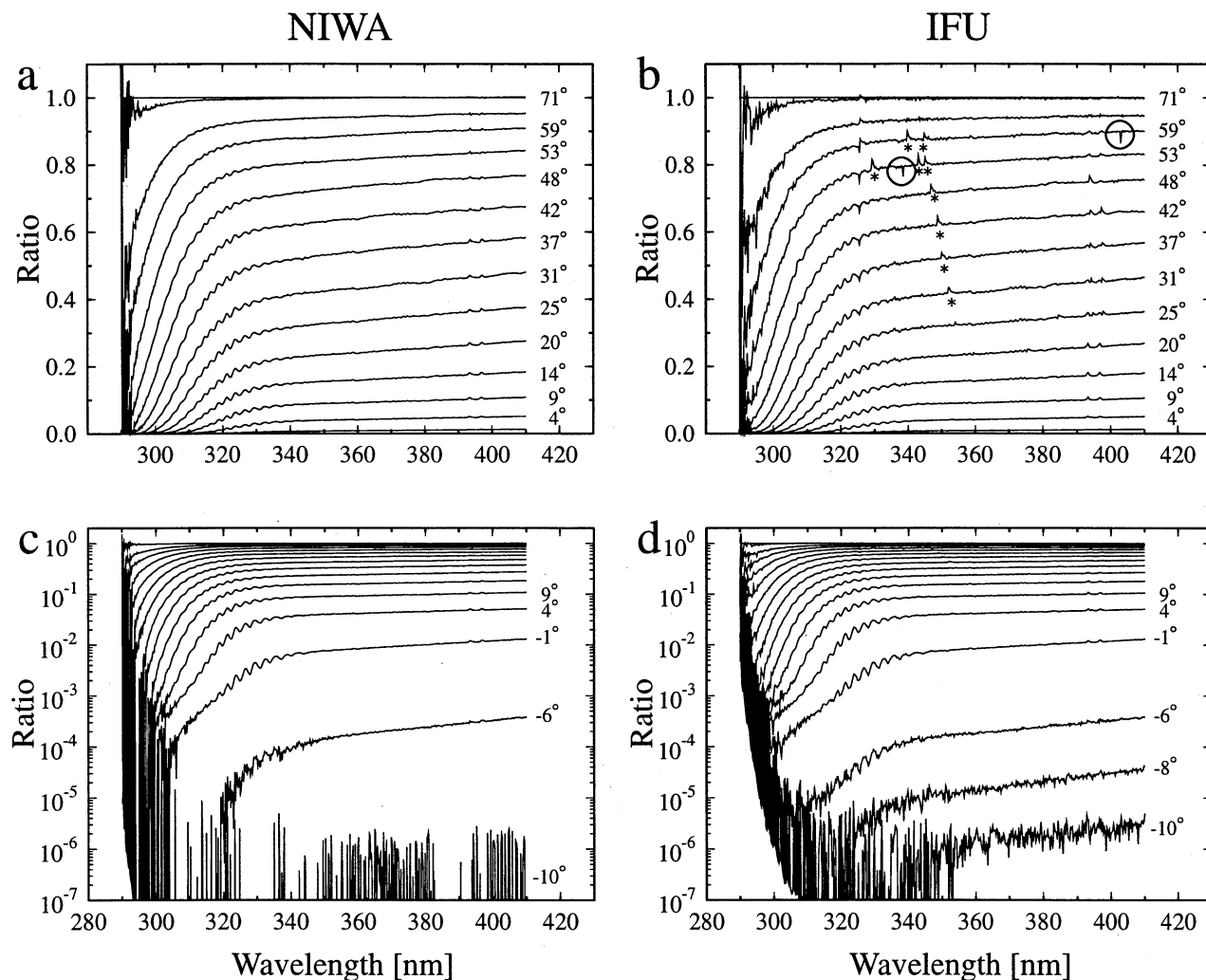
Figure 1. Ratios of spectra measured in the morning of July 5, 1997, in Nea Michaniona, Greece, to the noon spectrum on this day. The numbers on the right side of each ratio are the solar elevations at the start of each spectrum. (a) Ratio spectra of NIWA in linear presentation. (b) Ratio spectra of IFU in linear presentation. The features marked with an asterisk and a circle are caused by the instrument's amplifier; see text. (c) Ratio spectra of NIWA in logarithmic presentation. (d) Ratio spectra of IFU in logarithmic presentation. The lower noise level of the IFU instrument can be seen.

Because of rotational Raman scattering by O_2 and N_2 in the Earth's atmosphere, the depth of Fraunhofer lines is reduced (i.e., the "Ring" effect [*Grainger and Ring*, 1962]). Rotational Raman scattering occurs when, as a result of the interaction between the electric field and a rotating molecule, radiation is scattered with a change in frequency [*Fish and Jones*, 1995]. The "filling-in" of Fraunhofer lines by the Ring effect is most clearly apparent in the strong Fraunhofer lines at 393 and 397 nm (the Calcium doublet). At lower solar elevations, the contribution of scattered radiation increases, and therefore the Ring effect becomes more pronounced. This leads to the two small peaks at 393 and 397 nm that are visible in the ratio plots of both instruments. The Ring effect is slightly less prominent at high-altitude stations because there scattered radiation contributes less to global irradiance.

4. Inspection of Instrument Performance

Instrumental problems in both instruments were discovered by the presented method. By further investigations their causes could be identified.

The features marked with an asterisk in the linear plots of IFU were found to be caused by a change of the instrument's preamplifier stage. The small dips apparent at all ratios at 326 nm are produced by a switch of the amplifier during the noon spectrum. The problem is solved now by applying a longer settle time of some seconds after a change of the two amplifier stages.

The two dips marked with a circle were found by the method as well. Their reason is an interference of the control unit for the monochromator's stepper motors with the instrument's lock-in amplifier. By isolating both circuits, the spikes disappeared.

A dynamical range of almost six orders of magnitude can be discerned from the logarithmic ratio plots of both instruments. The noise level of the IFU spectroradiometer is lower than that of the NIWA system: For wavelengths above 360 nm, the IFU ratio for -10° solar elevation lies above the noise level, which is not the case for the corresponding NIWA ratio. The NIWA instrument operating at the SUSPEN campaign had just been constructed and suffered from excess electrical noise caused by the high-frequency current in the wavelength drive stepper motor that was coupled into the 20 bit analog to digital converter electronics because of a ground loop. The dynamic range was subsequently increased by removing the ground loop.

Figure 2 shows ratio spectra of the IFU instrument for a rainy day where the Sun was always hidden by clouds. Again, the ratios were formed from the morning spectra using the noon spectrum as the reference. Because there were no days with clouds during the SUSPEN intercomparison, the data were taken from measurements conducted at August 8, 1997, during the 1997 German intercomparison of spectroradiometers [Seckmeyer et al., 1998]. Figure 2 demonstrates that ratio spectra are also a useful quality control tool for cloudy days. Structures caused by ozone absorption, the Ring effect, and the lock-in amplifier (dip at 404.75 nm in the 57° spectrum) can clearly be identified. Because of changing cloud conditions, the ratios are irregularly curved and there is no systematic dependence on solar elevation.

5. Comparison with Model Calculations

In the following, the measurements of both instruments on July 5 will be compared with results from the pseudospherical version of the radiative transfer model UVSPEC [Dahlback and Stamnes, 1991; Mayer et al.,
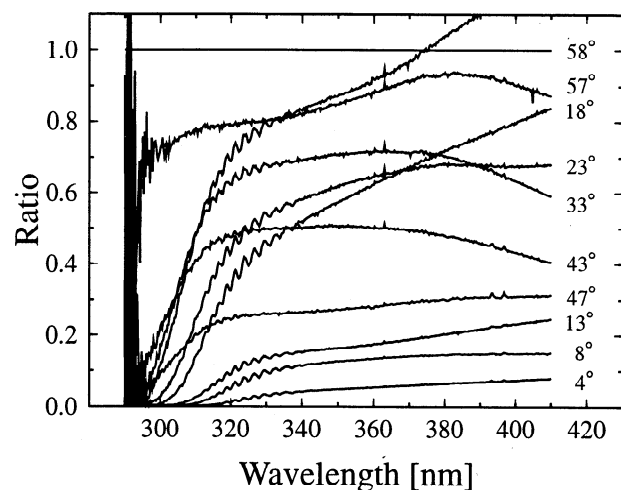
Figure 2. Ratios of spectra measured in the morning of August 8, 1997, in Garmisch-Partenkirchen, Germany, to the noon spectrum on this day. The numbers on the right side of each ratio are the solar elevations at the start of each spectrum. The ratios are irregularly curved because of the influence of clouds.

1997]. In section 6, the model will then be used to quantify wavelength shifts in the measured spectra. A more detailed comparison of measurements with an IFU spectroradiometer and the UVSPEC model, covering also different atmospheric conditions, is given by Mayer et al. [1997].

Important input parameters of the model are the extraterrestrial spectrum, the total ozone column, and aerosol parameters. Two spectra were considered. The first was measured by the Solar Ultraviolet Spectral Irradiance Monitor (SUSIM) during the third space shuttle mission of the Atmospheric Laboratory for Applications and Science (ATLAS 3) [Kaye and Miller, 1996]. The original spectrum was obtained from the ftp server susim.nrl.navy.mil and is given in vacuum wavelengths. For the comparison with the ground-based measurements, we shifted the spectrum to air wavelengths.

The second spectrum was the high-resolution "Kitt Peak spectrum" [Kurucz et al., 1984] that was obtained with the Fourier Transform Spectrometer at the McMath/Pierce Solar Telescope situated on Kitt Peak, Arizona. The original spectrum is given in air wavelengths. Since the spectrum is ground-based, it was modified to account for atmospheric absorptions. Differences in the SUSIM/ATLAS 3 and Kitt Peak spectra have been previously discussed in detail [Pfister et al., 1997].

The ozone column on July 5 was 300 Dobson units (DU) (1 DU = 2.69×10^{16} molecules/cm^2). The atmospheric aerosol was parameterized with Ångström's turbidity formula [Iqbal, 1983]. The Ångström parameters α and β were calculated from the aerosol optical depths at 340 and 500 nm, both measured with a Microtops II Sunphotometer from Solar Light Co. Finally, the model results were convolved with the slit function of the IFU instrument of bandwidth 0.58 nm full width at half maximum (FWHM), which was determined with a HeCd laser at 325 nm. Thus model values of global spectral irradiance were calculated at each data point measured by the IFU spectroradiometer on July 5.

In Figure 3, the ratio of the solar spectrum measured at noon by the IFU instrument to the corresponding model spectrum is depicted. If the SUSIM/ATLAS 3 spectrum is used for the model (top), measurement and model agree to within ±12% for all wavelengths above 305 nm. There is considerable "noise" apparent in the ratio. Among other factors, this can be caused by (1) small wavelength shifts in either the measurement or the extraterrestrial spectrum used as input of the model, (2) small differences in the actual slit function of the instrument and the function used to convolve the model spectrum, and (3) noise occurring during the radiometric calibration of either the IFU spectroradiometer or SUSIM/ATLAS 3.

When the Kitt peak spectrum is used as input of the model (bottom of Figure 3), the noisy structures present in the measurement/model ratio are similar in magnitude but generally different in detail. Additionally, the Kitt Peak spectrum appears to have anomalous values near 325 nm. In both the top and bottom of Figure 3, the asymmetry near the Ca-doublet is similar and indi-
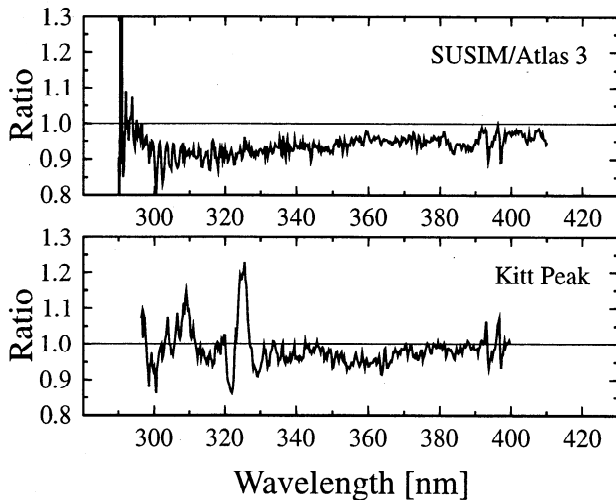
Figure 3. Ratio of spectral irradiance measured by IFU at noon of July 5 to the corresponding model spectrum: (top) model based on the extraterrestrial spectrum SUSIM/ATLAS 3 and (bottom) model based on the Kitt Peak spectrum.

cates a small systematic wavelength difference of about 0.03 nm between the IFU instrument and the reference spectra.

The structures in both ratios of Figure 3 are typical for ratios between measurements and models and document a fundamental difficulty when models are used for QC of spectral measurements: Many instrumental features mentioned in section 4 are masked, which is not the case if the method presented in this publication is applied.

6. Detection of Wavelength Errors

On the basis of the experience of previous intercomparison campaigns, wavelength errors of several tenths of a nanometer are common for many spectrometers [*Gardiner et al.*, 1993]. We first investigated the effect of a wavelength shift of 0.25 nm by deliberately shifting a noon spectrum of the IFU instrument by one sample point (= 0.25 nm) to longer wavelengths before taking the ratio with the correctly aligned spectrum. The result is shown in Figure 4, which also includes the ratio of the corresponding shifted and unshifted model spectra based on the SUSIM/ATLAS 3 spectrum. Both ratios show strong wavelength dependent variations that reach values of up to 1.4 in the vicinity of the strongest Fraunhofer lines. On average, the ratios are between 0.8 and 1.2. The fluctuations in the measurement ratio and model ratio are similar, though not identical, as discussed above. Their differences are shown as a residual in the lower curve, referred to the right axis.

Although imperfect, the agreement between the modeled ratios and the measurement ratios proved to be sufficiently accurate to use the model to make a quantitative analysis of structures in ratio plots due to wavelength shifts. In a first step, we looked at the two peaks, labeled R_{max} and R_{min} in Figure 4, which are caused by the combined influence of the deliberately ap-

plied wavelength shift of 0.25 nm and the Ca H Fraunhofer line at 396.85 nm. In general, the extent of both peaks depends not only on the magnitude of the wavelength shift but also on the resolution of the given spectrum. To quantify these dependencies, we convolved a high-resolution UVSPEC model spectrum with triangular slit functions of different bandwidths before forming the ratios of shifted and unshifted spectra. From these ratios, the maximum and minimum values R_{max} and R_{min} near the Ca H line were extracted. In Figure 5, R_{max} and R_{min} are shown for wavelength shifts between -0.5 and $+0.5$ nm, where the underlying spectra had been convolved with triangular slit functions of 0.3, 0.5, 0.7, 1.0, and 2.0 nm FWHM. Figure 5 shows that spectra with high resolution lead to higher values of R_{max} than spectra with low resolution. For example, a wavelength shift of 0.1 nm applied to measurements of an instrument with 0.3 nm resolution would lead to a maximum peak in the accompaning ratio spectrum of $R_{max} = 1.27$, whereas the same shift for an instrument with 2.0 nm resolution would cause a peak value only of 1.03. Thus features in ratio spectra of high-resolution instruments are more pronounced. Figure 5 illustrates that the peak values vary approximately linearly with the magnitude of the shift. However, for larger shifts or for spectra with small resolution, the deviation from the linear relationship becomes prominent. For small wavelength shifts, the plot is quite symmetrical with respect to positive and negative shifts.

After studying in detail the effect of wavelength shifts and spectral resolution on ratio spectra in the vicinity of the Ca II line, we compared the change of wavelength-correlated structures in the ratio plots of the IFU and NIWA instrument during a day with corresponding structures in model ratios. In Figure 6a, ratio spectra based on the model results are plotted for the same
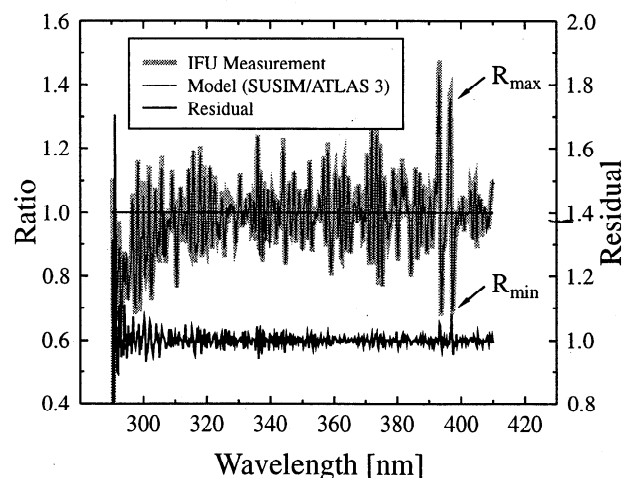
Figure 4. Effect of wavelength shifts on spectral irradiance: (very thick line, left axis) spectral irradiance measured by IFU at noon of July 5 and deliberately shifted by 0.25 nm and then divided by the unshifted spectrum, (thin line, left axis) ratio of the corresponding shifted and unshifted model spectra, and (thick line, right axis) residual of both ratios, that is, measured ratio/modeled ratio.
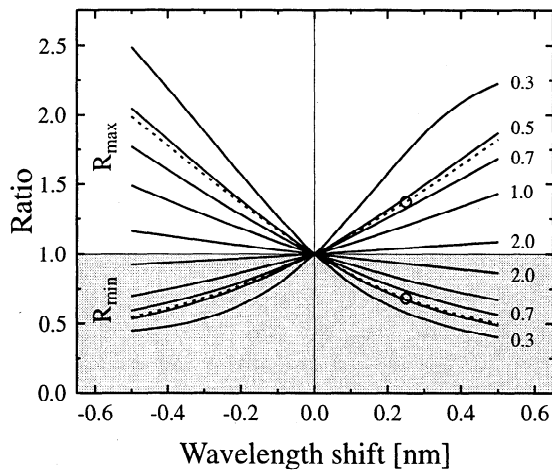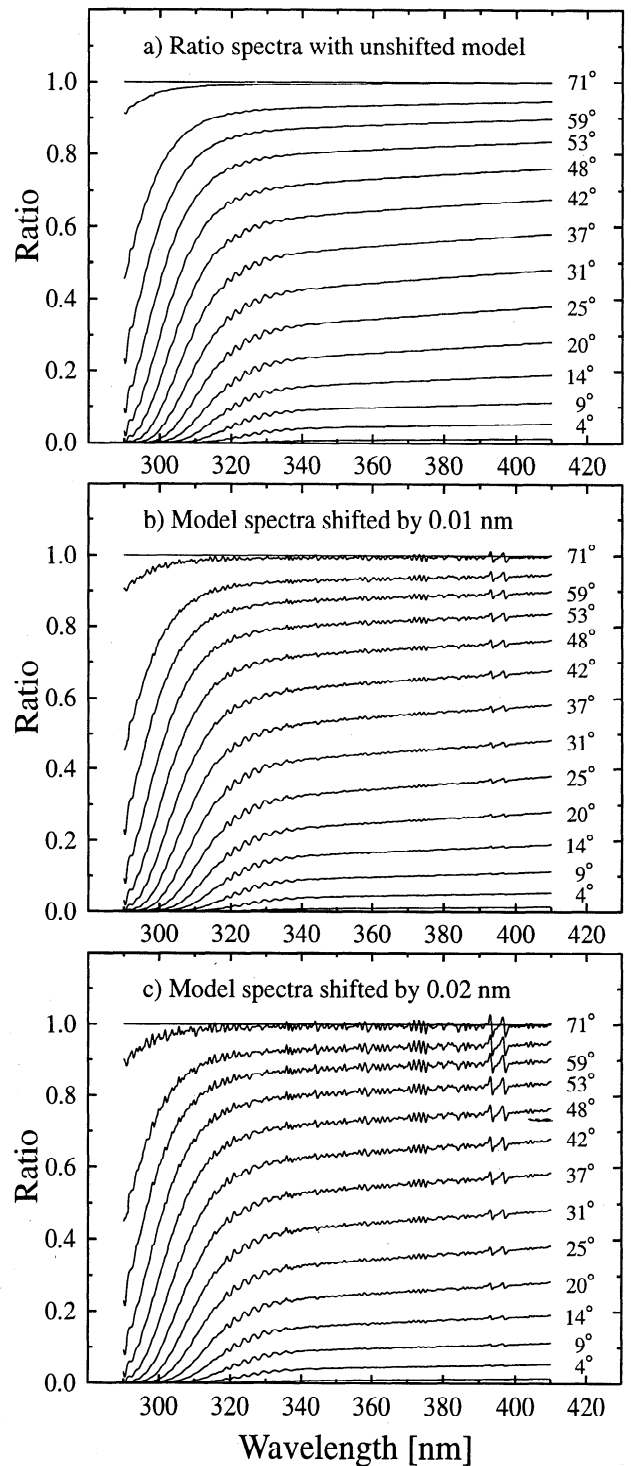
Figure 5. Effect of wavelength shifts and spectral resolution on the peaks R_{max} and R_{min} that are visible in ratio spectra near 397 nm. The wavelength dependence of R_{max} and R_{min} (shaded area) is plotted for five model spectra convolved with triangular slit functions of 0.3, 0.5, 0.7, 1.0, and 2.0 nm FWHM; see numbers on the right side of the curves. The dashed line is based on a model spectrum that was convolved with the measured slit function of the IFU instrument. The two circles in the plot mark the peak values for the IFU instrument for a shift of 0.25 nm, which were already highlighted in Figure 4.

derived from satellite data. An appropriate implementation is described by *Slaper et al.* [1995]. Such methods are also suitable for determining the stability of an instrument's wavelength setting over a day. However, the output of these correlation methods is usually a wavelength shift averaged over a certain wavelength region, for example, over 16 nm in the case of the algorithm pre-

solar elevations as in Figure 1. Apart from the structure from the ozone cross section, the ratios are smooth. Since Raman scattering is not taken into consideration by the model, no features at the Calcium lines are visible. Figure 6b was constructed by applying a shift of 0.01 nm to all model spectra, then dividing by the unshifted noon spectrum. A shift of 0.01 nm is near the limit that most spectroradiometers used for solar UV measurements can resolve. However, even for this small shift, variations in the ratio spectra are apparent, especially in the wavelength range between 370 and 400 nm. If the model spectra are shifted by 0.02 nm (Figure 6c), fluctuations can be clearly seen over the whole spectral range.

By comparing the model-based ratio plots of Figures 6b and 6c with the ratio spectra in Figure 1, it can be concluded that any changes of the wavelength calibrations during the morning of July 5, of both the NIWA and the IFU instruments, are below 0.02 nm and probably even less than 0.01 nm. Note that the wavelength errors manifest themselves as error functions about the line centers of the Fraunhofer lines. For example, in Figures 6b and 6c, the error is positive on the short-wavelength side and negative on the long-wavelength side of the line. This contrasts with the Ring effect (see Figure 1), which is more symmetrical about the line and so produces single-peak features at line centers.

As an alternative to our method, the wavelength calibration of an instrument can be checked by correlating the Fraunhofer structure in segments of the measured spectra with the respective structure in a reference solar spectrum, for example, an extraterrestrial spectrum

Figure 6. Effect of wavelength shifts on ratio plots. (a) Ratio plot based on unshifted model spectra. (b) Ratios of model spectra shifted by 0.01 nm and the unshifted noon spectrum. (c) Ratios of model spectra shifted by 0.02 nm and the unshifted noon spectrum.

sented by *Slaper et al.* [1995]. In contrast, the method proposed in this paper allows an estimate to be made of the wavelength stability on a 1 nm scale. A second disadvantage of correlation methods is that both structures in the ozone cross section, which interfere with the Fraunhofer lines, and electronic noise in the measured spectra can lead to erratic results. We concluded that the latter is the case when the method of *Slaper et al.* [1995] was applied to the measurements of the NIWA instrument in Greece.

7. Conclusions

The benefits of the method presented can be summarized as follows:

1. It is very sensitive to spikes and similar instrumental features because no interference with the Sun's Fraunhofer lines or features produced by the calibration need to be considered.

2. It is easy to apply. Simple spread sheet software without special mathematics is sufficient.

3. The stability of the wavelength calibration can be checked visually, without the need to determine the stability by correlation methods.

4. Features can be detected on a "1 nm scale."

5. The method can be recommended as a general QA/QC tool for UV monitoring.

References

Bernhard, G., and G. Seckmeyer, New entrance optics for solar spectral UV measurements, *Photochem. Photobiol.,* 65(6), 923-930, 1997.

Bernhard, G., A. Moise, B. Mayer, and G. Seckmeyer, Measurements of spectral solar UV irradiance in tropical Australia, *J. Geophys. Res., 102*(D7), 8719-8730, 1997.

Dahlback, A., and K. Stamnes, A new spherical model for computing the radiation field available for photolysis and heating at twilight, *Planet. Space Sci., 39,* 671-683, 1991.

Fish, D. J., and R. L. Jones, Rotational Raman scattering and the ring effect in zenith-sky spectra, *Geophys. Res. Lett., 22*(7), 811-814, 1995.

Gardiner, B. G., et al., European intercomparison of ultraviolet spectroradiometers, *Environ. Technol., 14,* 25-43, 1993.

Grainger, J. F., and J. Ring, Anomalous Fraunhofer line profiles, *Nature, 193,* 762, 1962.

Iqbal, M., *An Introduction to Solar Radiation,* Academic, San Diego, Calif., 1983.

Kaye, J. A., and T. L. Miller, The ATLAS series of shuttle missions, *Geophys. Res. Lett., 23*(17), 2285-2288, 1996.

Kreher, K., P. V. Johnston, S. W. Wood, and J. G. Keys, Ground-based observations of OClO, BrO and NO2 during 1995 at Arrival Heights (77.8°S) Antarctica, in *Proceedings of the XVIII Quadrennial Ozone Symposium, L'Aquila, Italy,* edited by R. D. Bojkov and G. Visconti, pp. 217-220, Edigrafital S.p.A., S. Atto (TE), Italy, 1997.

Kurucz, R. L., I. Furenlid, J. Brault, and L. Testerman, Solar flux atlas from 296 to 1300 nm, in *National Solar Observatory Atlas No. 1,* Harvard. Univ. Univ. Publ., Sunspot, N. M., 1984.

Mayer, B., A. Kylling, and G. Seckmeyer, Systematic long-term comparison of spectral UV measurements and UVSPEC modeling results, *J. Geophys. Res., 102*(D7), 8755-8767, 1997.

McKenzie, R. L., and P. V. Johnston, Stratospheric ozone observations simultaneous with NO2 at 45°S, *Geophys. Res. Lett., 10*(4), 337-340, 1983.

McKenzie, R. L., M. Blumthaler, C. R. Booth, S. B. Diaz, J. E. Frederick, T. Ito, S. Madronich, and G. Seckmeyer, Surface ultraviolet radiation, in *Scientific Assessment of Ozone Depletion: 1994,* edited by the World Meteorological Organization, chap. 9, pp. 9.1-9.22, U. N. Environ. Programme, Nairobi, 1994.

McMahon, B. B., and E. L. Simmons, Ground based measurements of atmospheric NO2 by differential optical absorption, *Nature, 287,* 710-711, 1980.

Pfister, G., E. Putz, G. Bernhard, G. Seckmeyer, and B. Mayer, Comparison of high resolution spectral UV measurements with DISORT model results using different extraterrestrial spectra, in *IRS '96: Current Problems in Atmospheric Radiation,* edited by W. L. Smith and K. Stamnes, pp. 938-941, A. Deepak, Hampton, Va., 1997.

Seckmeyer, G., et al., Comparison of spectral UV-radiation measurement systems, *Applied Opt., 33*(33), 7805-7812, 1994.

Seckmeyer, G., et al., Geographical differences in the UV measured by intercompared spectroradiometers, *Geophys. Res. Lett., 22*(14), 1889-1892, 1995.

Seckmeyer, G., G. Bernhard, B. Mayer, and R. Erb, High accuracy spectroradiometry of solar ultraviolet radiation, *Metrologia, 32*(6), 697-700, 1996.

Seckmeyer, G., B. Mayer, G. Bernhard, *The 1997 Status of Solar UV Spectroradiometry in Germany: Results From the National Intercomparison of UV Spectroradiometers, Garmisch-Partenkirchen, Germany,* 166 pp., Shaker, Aachen, Germany, 1998.

Slaper, H., H. A. J. M. Reinen, M. Blumthaler, M. Huber, and F. Kuik, Comparing ground-level spectrally resolved solar UV measurements using various instruments: A technique resolving effects of wavelength shift and slit width, *Geophys. Res. Lett., 22*(20), 2721-2724, 1995.

Webb, A. R. (Ed.), Advances in solar ultraviolet spectroradiometry, air pollution research report 63, Off. for Off. Publ. of the Eur. Communities, Luxembourg, 1997.

G. Bernhard, Biospherical Instruments Inc., 5340 Riley Street, San Diego, CA 92110-2621. (e-mail: bernhard@biospherical.com)

G. Seckmeyer, Fraunhofer IFU, Kreuzeckbahnstraße 19, D-82467 Garmisch-Partenkirchen, Germany. (e-mail: seckmeyer@ifu.fhg.de)

R. L. McKenzie and P. V. Johnston, National Institute of Water and Atmospheric Research (NIWA), Lauder, PB 50061 Omakau, Central Otago, New Zealand. (e-mail: r.mckenzie@niwa.cri.nz; p.johnston@niwa.cri.nz)